PCCP

Accepted Manuscript

This is an *Accepted Manuscript*, which has been through the Royal Society of Chemistry peer review process and has been accepted for publication.

Accepted Manuscripts are published online shortly after acceptance, before technical editing, formatting and proof reading. Using this free service, authors can make their results available to the community, in citable form, before we publish the edited article. We will replace this *Accepted Manuscript* with the edited and formatted *Advance Article* as soon as it is available.

You can find more information about *Accepted Manuscripts* in the Information for Authors.

Please note that technical editing may introduce minor changes to the text and/or graphics, which may alter content. The journal's standard Terms & Conditions and the Ethical guidelines still apply. In no event shall the Royal Society of Chemistry be held responsible for any errors or omissions in this *Accepted Manuscript* or any consequences arising from the use of any information it contains.

ROYAL SOCIETY OF CHEMISTRY

www.rsc.org/pccp

Liquid Crystal Seed Nucleates Liquid-Solid Phase Change in Ceria Nanoparticles

Thi X. T. Sayle, Lewis W. L. Sayle and Dean C. Sayle

School of Physical Sciences, University of Kent, Canterbury, CT2 7NZ, UK *d.c.sayle@kent.ac.uk

ABSTRACT

Molecular Dynamics (MD) simulation was used to explore the liquid-solid (crystal) phase change of a ceria nanoparticle. The simulations reveal that the crystalline seed, which spontaneously evolves and nucleates crystallisation, is a liquid rather than a solid. Evidence supporting this concept includes: (a) only 3% of the total latent heat of solidification had been liberated after 25% of the nanoparticle had (visibly) crystallised. (b) Cerium ions, comprising the (liquid) crystal seed had the same mobility as cerium ions comprising the amorphous regions. (c) Cerium ion mobility only started to reduce (indicative of solidification) after 25% of the nanoparticle had crystallised. (d) Calculated Radial Distribution Functions (RDF) revealed no long-range structure when 25% of the nanoparticle had (visibly) crystallised. We present evidence that the concept of a liquid crystal seed is more general phenomenon rather than applicable only to nanoceria.

INTRODUCTION

Classical Nucleation Theory (CNT) describes the process underpinning a phase change from a liquid phase to a solid (crystal) phase[1] and is central to the evolution of a material microstructure, which governs its physical, chemical and mechanical properties. The microstructure includes, for example, the polymorphic crystal structure (polymorphic forms of carbon include graphite and diamond, which have very different properties); morphology and the surfaces exposed with implications for the catalytic activity;[2] dislocations and grain-boundaries, which impact upon the mechanical properties;[3] point defects, which are pivotal to electronic and ionic conductivity with application for solid oxide fuels[4] and catalysis.[5]

Understanding, at the atom level, of the mechanism underpinning crystallisation, whether from solution[6] or the freezing of a liquid,[7] has been the subject of intense scrutiny spanning many decades because such understanding will facilitate the ability to control the crystallisation and realise desirable (application) microstructures for targeted application. Moreover, with the recent discovery

Physical Chemistry Chemical Physics Accepted Manuscript

of nanoparticle-mediated crystallization theory (non-classical crystallisation) the field remains the subject of intense scientific interest and scrutiny.[8]

Experimentally, it is very difficult to characterise, with atom-level resolution, the time resolved homogeneous crystallisation of a material via the spontaneous evolution of a crystalline nucleating seed,[9] and therefore computer simulation can provide unique insight.[10]

Atomistic simulation has been used to explore the freezing of water,[11] metals[12] and nanoparticles,[13] crystallisation from solution,[6] and biotemplated crystallisation.[14] However, a major obstacle with simulating crystallisation directly, using Molecular Dynamics (MD) simulation, are the high energy barriers associated with evolving a solid crystalline seed starting from an amorphous precursor. In particular, MD is only able to simulate small windows in time – typically of the order of nanoseconds, which reduces the probability of simulating the potential hypersurface sufficiently to capture the spontaneous evolution of the seed within the duration of the simulation. Accordingly, accelerated dynamics has been used to overcome such limitations.[14] However, as Anwar and Zahn report: 'you don't gain something for nothing' and the approximations of accelerating the dynamics means that certain choices with regards to the final state and pathway must be made, which can obscure alternative pathways that the system may take during the crystallisation process.[10]

Here, we use molecular dynamics simulation to explore directly the nucleation and crystal growth of ceria nanoparticles, which are widely exploited in applications spanning: catalysis[15] to nanomedicine.[16]

METHODS

The calculations presented in this study are based upon the Born model of the ionic solid, where the energy of the system is given by:

$$E(r_{ij}) = \sum_{ij} \frac{Q_i Q_j}{4\pi\varepsilon_o r_{ij}} + \sum_{ij} A\exp\left(\frac{-r_{ij}}{\rho}\right) - Cr_{ij}^{-6},$$

the first term represents the Coulombic interaction between ion *i* of charge Q_i and ion *j* of charge Q_j, which are a distance r_{ij} apart. The second term is of the Buckingham form, which is particularly effective in representing ionic solids. Model parameters, used to describe CeO_2 and water together with the interactions between ceria and water were taken from ref. [[17]]. The Molecular Dynamical simulations were performed using the DLPOLY code.[18]

Physical Chemistry Chemical Physics Accepted Manuscript

To simulate solidification, a nanoparticle of ceria was first melted by heating it at a temperature above its melting point and then solidified by cooling the nanoparticle at a temperature below its melting point using MD simulation; analysis of the dynamical trajectories of the ions, using analytical and molecular graphical techniques, was then used to elucidate the mechanisms underpinning the solidification process.

Specifically, a cube of ceria comprising 15972 atoms was cleaved from the parent bulk material and melted by performing MD simulation at 6500K using a 0.001ps time-step. After 14,000 cycles of MD simulation (14ps) the nanoparticle was observed to be liquid phase. The model nanoparticle was then immersed in water and the temperature was reduced to 2390K. MD simulation was performed for 2500ps using a 0.003ps time-step, during which time the nanoparticle solidified.

The MD simulations were performed using an NPT ensemble (constant **N**umber of particles, constant **P**ressure, constant **T**emperature). The pressure was set to zero with thermostat and barostat relaxation times of 0.1 and 0.5ps respectively; a real-space potential cut-off of 10.0Å and an Ewald precision of 10^{-6} was employed.

We note that the water molecules were held fixed during the crystallisation, which is unphysical. However, the reason for immersing the nanoparticle in water was not to simulate the influence of an aqueous environment on the solidification; rather it was to ensure that the nanoparticle did not rotate during the solidification. If the nanoparticle is allowed to solidify in vacuum, the latent heat of solidification can sometimes be converted into rotational energy. Such rotation of the nanoparticle would prevent reliable extraction of the individual atom velocities from the simulation because the velocities of the ions would include a contribution from the rotational velocity. The role of the water was therefore wholly to provide a cavity in which the nanoparticle can solidify without rotating. The system pressure during the simulation was calculated to be 0 ± 0.05 kbar and therefore the cavity does not constrain the nanoparticle to crystallise under (high) pressure.

The chosen temperature (2390K) is critical to the simulation of the solidification. In particular, preliminary simulations revealed that at 2800K the nanoparticle was molten but as the temperature was reduced to 2600K the nanoparticle crystallised. The melting point of the nanoparticle (associated with the potential model) therefore lies between 2600 and 2800K. Preliminary simulations revealed that the speed of crystallisation increases with increasing temperature. We propose that at 2600K the crystallisation speed is higher compared to crystallisation at a lower temperature because at the higher temperature there is a higher probability that individual ions have sufficient energy to overcome the barriers associated with locating to lattice sites to propagate

Physical Chemistry Chemical Physics Accepted Manuscript

the crystallisation (exploring configurational space). Conversely, a fast speed of crystallisation reduces the size of the trajectory data, which emanates from the MD simulation; the trajectory data comprises the positions, velocities and accelerations of the ions as a function of time. Accordingly, to better 'observe' and understand the solidification, a (supercooled) temperature of 2390K was chosen, which reduced the speed of the crystallisation, increased the size of the trajectory data and hence increased the amount of mechanistic detail that could be extracted from the trajectory data (albeit at increased computational cost); the simulation required about 50,000 cpu hours.

RESULTS

In this section, we analyse the trajectory data using analytical and molecular graphical techniques to: characterise the atomistic structure of the nanoparticle as it crystallises; calculate the heat of solidification emanating from the nanoparticle; characterise the atomistic structure of the nanoparticle during the embryonic stages of solidification; calculate the mobility of the cerium cations and oxygen anions during solidification; determine the long-range structural order of the nanoparticle during solidification and elucidate the mechanisms associated with the propagation of crystallisation - emanating from the nucleating seed.

Crystallisation The configuration energy, average cerium ion velocity and structure of the CeO_2 nanoparticle, calculated as a function of time, are shown in fig 1. The figure reveals that the nanoparticle is initially liquid, fig 1(b), and then at a particular instance in time a crystalline seed *spontaneously* evolves within the amorphous sea of ions, fig 1(c). The seed then grows in size, fig 1(d-f) until the whole nanoparticle is crystalline, fig 1(g).

Latent Heat of Solidification During the whole simulation, the configurational energy decreases by 180kJ/kg, which reflects the latent heat of solidification. At 675ps, about 25% of the nanoparticle is observed to be crystalline, fig 1(e). Accordingly, one might expect that the decrease in configurational energy at 675ps would be 45kJ/Kg or 25% of the total latent heat. However, the decrease in configurational energy at this point is only 6kJ/kg or 3% of the total latent heat of solidification. This suggests that the crystalline seed may not exist as a solid.

Physical Chemistry Chemical Physics Accepted Manuscript

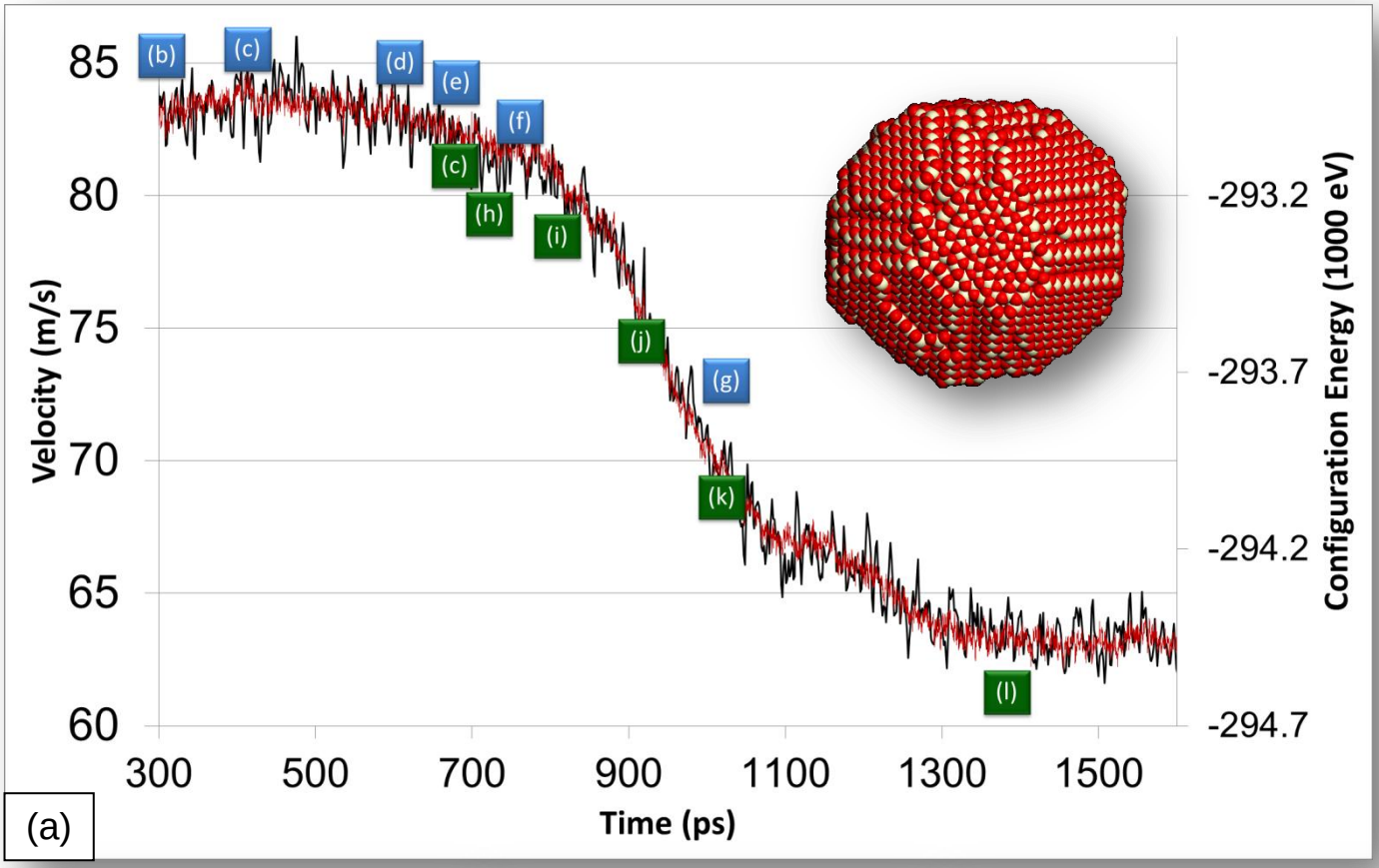

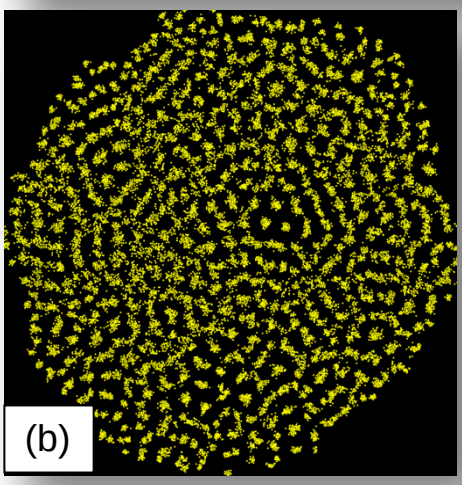

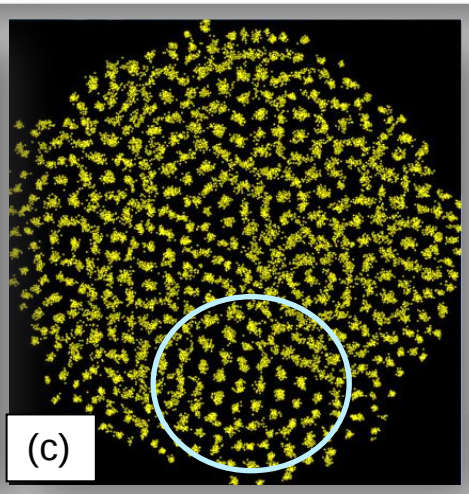

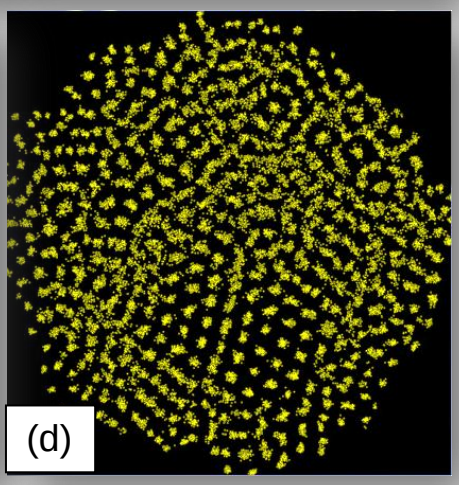

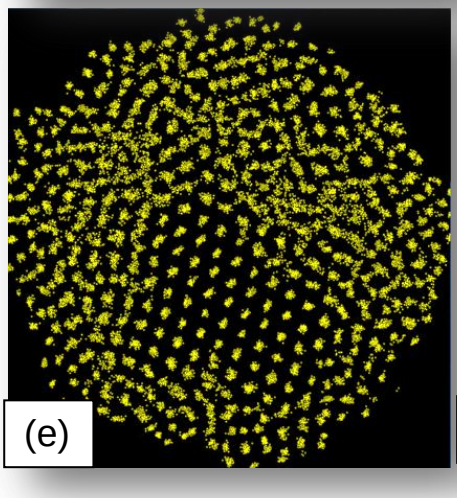

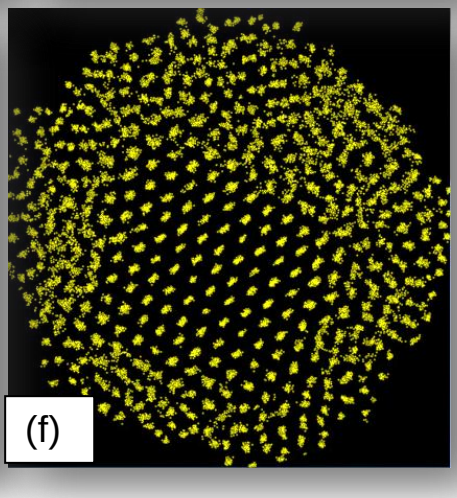

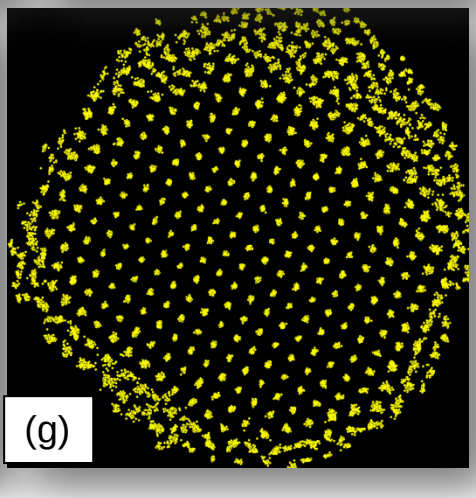

Physical Chemistry Chemical Physics Accepted Manuscript

Figure 1 (a) Average Ce ion velocity (red trace, first ordinate), configurational energy (black trace, second ordinate) of the CeO_2 nanoparticle, calculated as a function of time. Ce atom positions (yellow) comprising the nanoparticle, at selected times during the crystallisation, are shown in: (b) 300ps, (c) 415ps, (d) 600ps, (e) 675ps, (f) 750ps, (g) 1000ps. The configurational energy of each structure is annotated (blue labels) in (a). The fully crystallised CeO_2 nanoparticle is shown top right in (a); cerium is coloured white and oxygen is red. Green labels in (a) correlate to the solidification, fig 2.

Embryonic Stages of Solidification In fluorite-structured CeO_2, the energy barriers associated with Ce mobility are so high that Ce mobility within the lattice cannot be 'observed' using MD simulation. Accordingly, we used this criterion to determine the phase (liquid or solid) of the CeO_2. In particular, all Ce ions that are mobile during the MD simulation are deemed to be liquid phase. Specifically, the criterion for determining Ce mobility was to identify Ce ions, which escape their lattice site and move further than the nearest interstitial position. In fluorite-structured CeO_2 nanoparticle, the distance from a cerium lattice point to the nearest interstitial site is 1.35Å. If the material were a crystalline solid, the Ce ions would not be observed to escape their lattice sites and move past the nearest interstitial site under MD simulation because of the high associated energy barrier. Accordingly, to determine the onset of solidification, those cerium ions, which moved less than 1.5Å during a 75ps interval, were identified as ions comprising solid regions of the nanoparticle. The strategy enabled the spontaneous evolution, embryonic structure and growth of the *solid* phase to be mapped, fig 2, and can be usefully correlated with the configurational energy, fig 1(a); (green labels).

Physical Chemistry Chemical Physics Accepted Manuscript

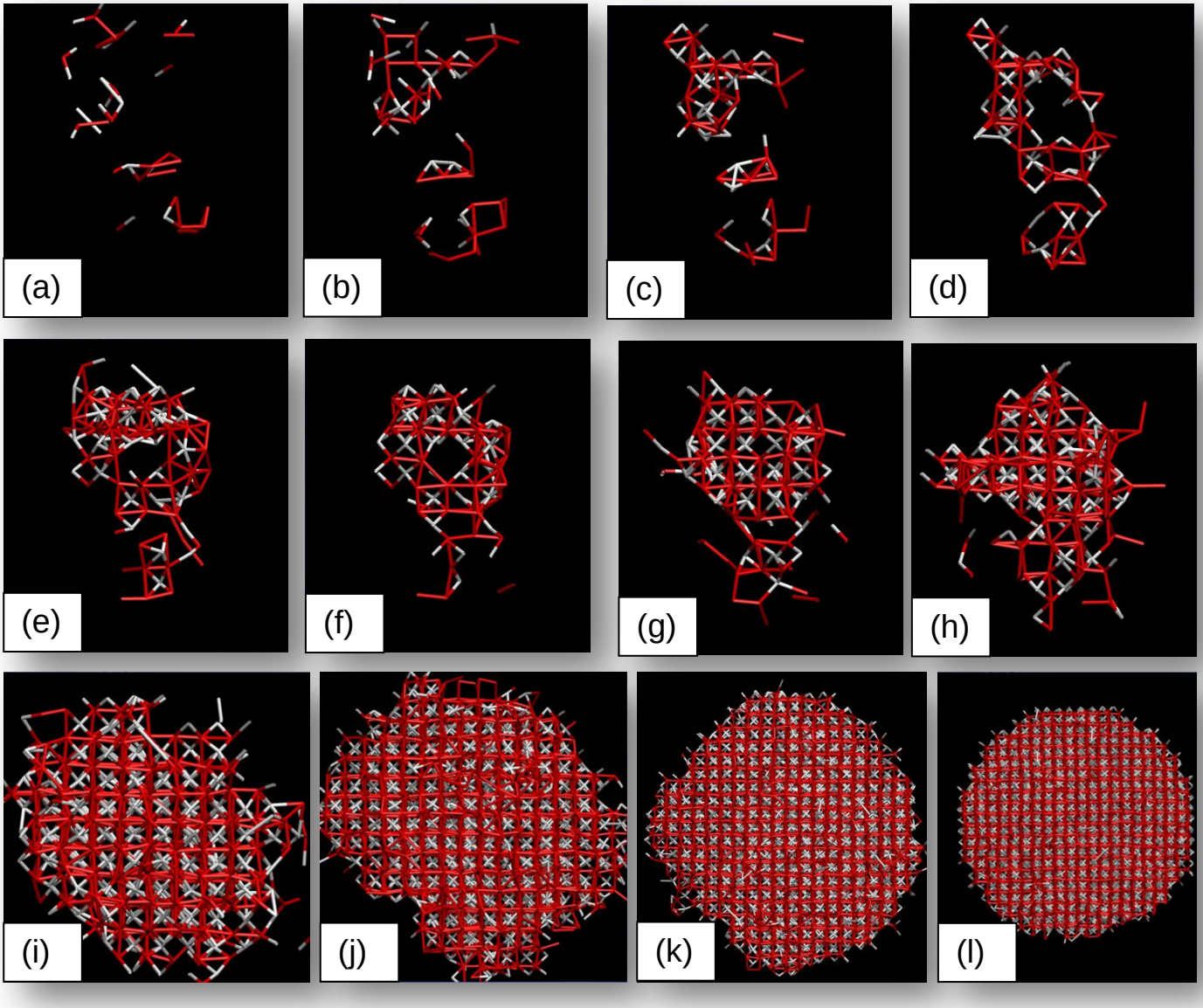

Figure 2 Spontaneous evolution, growth and embryonic structure of the solid crystalline seed as a function of time. (a) 665ps (b) 670ps (c) 675ps (d) 680ps (e) 685ps (f) 690ps (g) 700ps (h) 710ps (i) 800ps (j) 910ps (k) 1000ps (l) 1350ps. Ce ions are coloured white and oxygen is red. The configurational energies of the structures are indicated, green labels, in fig 1(a).

The structures, shown in fig 2, reveal that the onset of solidification occurs at about 665ps - no ions were identified to have mobilities of less than 1.5Å/75ps before this time. At 675ps, the fluorite structure becomes evident, fig 2(c). However, the size of the solid region at 675ps, fig 2(c), is much smaller than the crystalline region, fig 1(e), at 675ps. Indeed, a crystalline seed is visible as early as 415ps, fig 1(c), which is much earlier than the onset of solidification (665ps). The simulations therefore reveal that the crystalline seed, fig 1(c,d), is liquid. Moreover, analysis of the MD trajectory confirmed that the cations comprising the crystalline seed are able to diffuse and move between lattice sites.

Physical Chemistry Chemical Physics Accepted Manuscript

Ionic Mobility Cerium and oxygen Mean Square Displacements (MSD), calculated as a function of time, are shown in fig. 3. The onset of crystallisation (at 415ps, fig 1(c)) and the onset of solidification (665ps, fig 2(a)) are indicated on the figure using dashed lines. The gradient of the MSD trace, which reflects the ionic mobility, remains constant from before the onset of crystallisation up to about 700ps at which point over 25% of the nanoparticle is crystalline, fig 1(e, f). Accordingly, the mobility of ions comprising the crystalline region is commensurate with the mobility of ions comprising the amorphous regions because if the mobility of ions comprising the crystalline regions reduced, this would be reflected in a reduction in the gradient of the MSD trace. After 700ps, the MSD trace exhibits a reduction in the gradient indicating a reduction in the average cation mobility.

At about 1100ps, the gradient of the MDS trace, fig 3, shows a sharp discontinuity and indicates that the nanoparticle is entirely solid. We note that the gradient of the MSD trace above 1100ps is not zero; analysis of the cerium ion mobility, using molecular graphics, reveals that the residual mobility is attributed to Cerium ions moving on the surface of the nanoparticle.

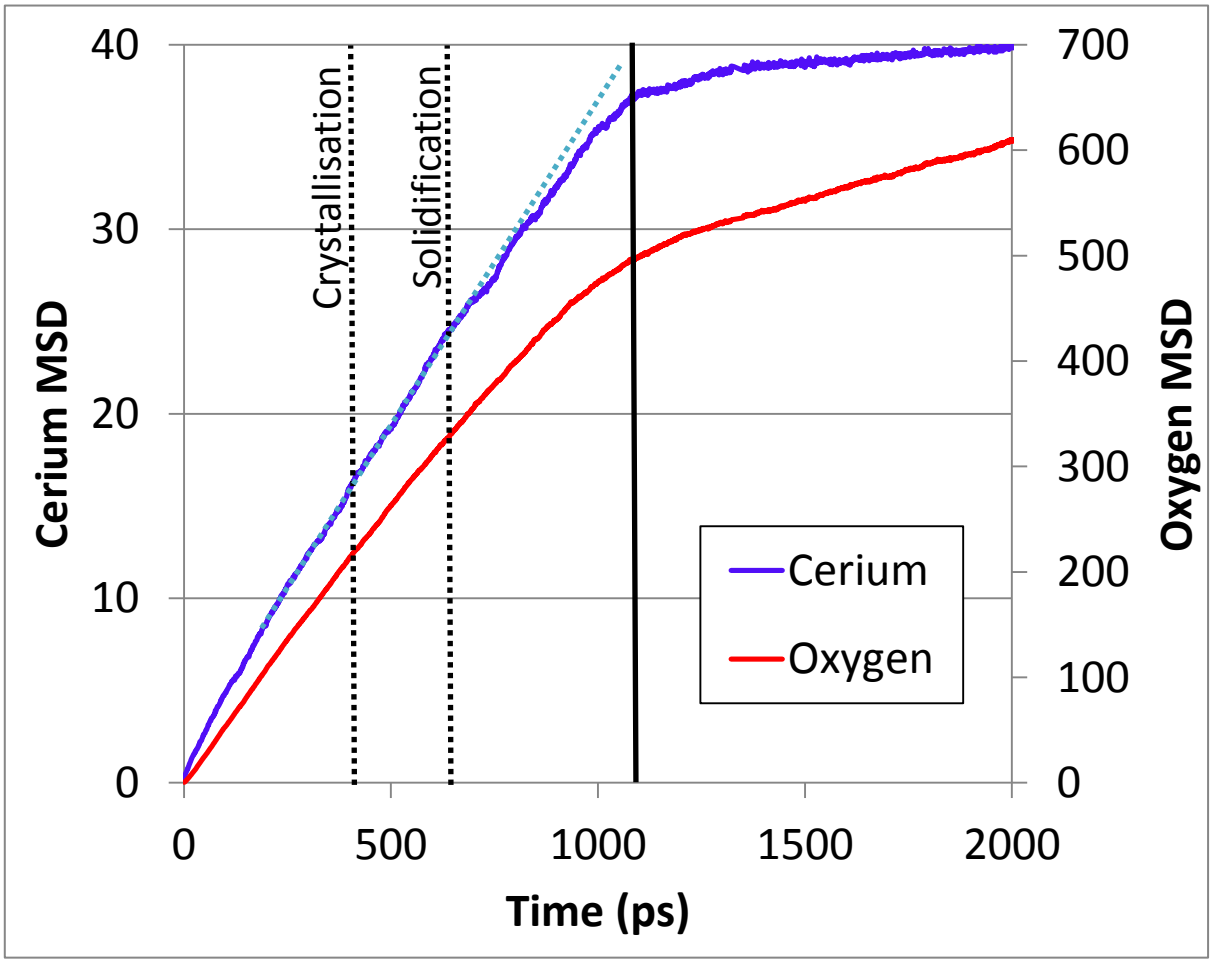

Physical Chemistry Chemical Physics Accepted Manuscript

Figure 3 Mean Square Displacements ($Å^2$) calculated as a function of time (ps). The light blue dashed line, superimposed over the cerium ion MSD trace, shows that the mobility of the cerium ions does not change during the period of time in which over 25% of the nanoparticle crystallises.

Nanoparticle Crystallinity To further identify the onset of solidification, the Ce-Ce, Ce-O and O-O Radial Distribution Functions (RDF) were calculated as a function of time. The RDF traces revealed evidence of the onset of long-range order (indicative of crystallinity) of the nanoparticle at about 900ps. In particular, fig 4 shows the next-nearest-neighbour Ce-Ce peak starting to emerge at 900ps. Prior to this time, the RDF traces are broad and commensurate with an amorphous (molten) structure. Conversely, 25% of the nanoparticle is (visually) crystalline at 675ps, fig 1(e). We attribute this anomaly, between the analytical appraisal of the crystallinity (via RDF) compared to the visual appraisal of the crystallinity, to the disorder of the crystalline seed. In particular, visually the ions appear to be located at lattice sites, but careful inspection reveals that the ions are somewhat disordered – analogous to a large thermal ellipsoid associated with each lattice site. Such disorder manifests within the RDF at the next-nearest-neighbour peak and beyond and therefore the long-range structure of the crystalline seed cannot be captured within the RDF because of the thermal ellipsoids.

Physical Chemistry Chemical Physics Accepted Manuscript

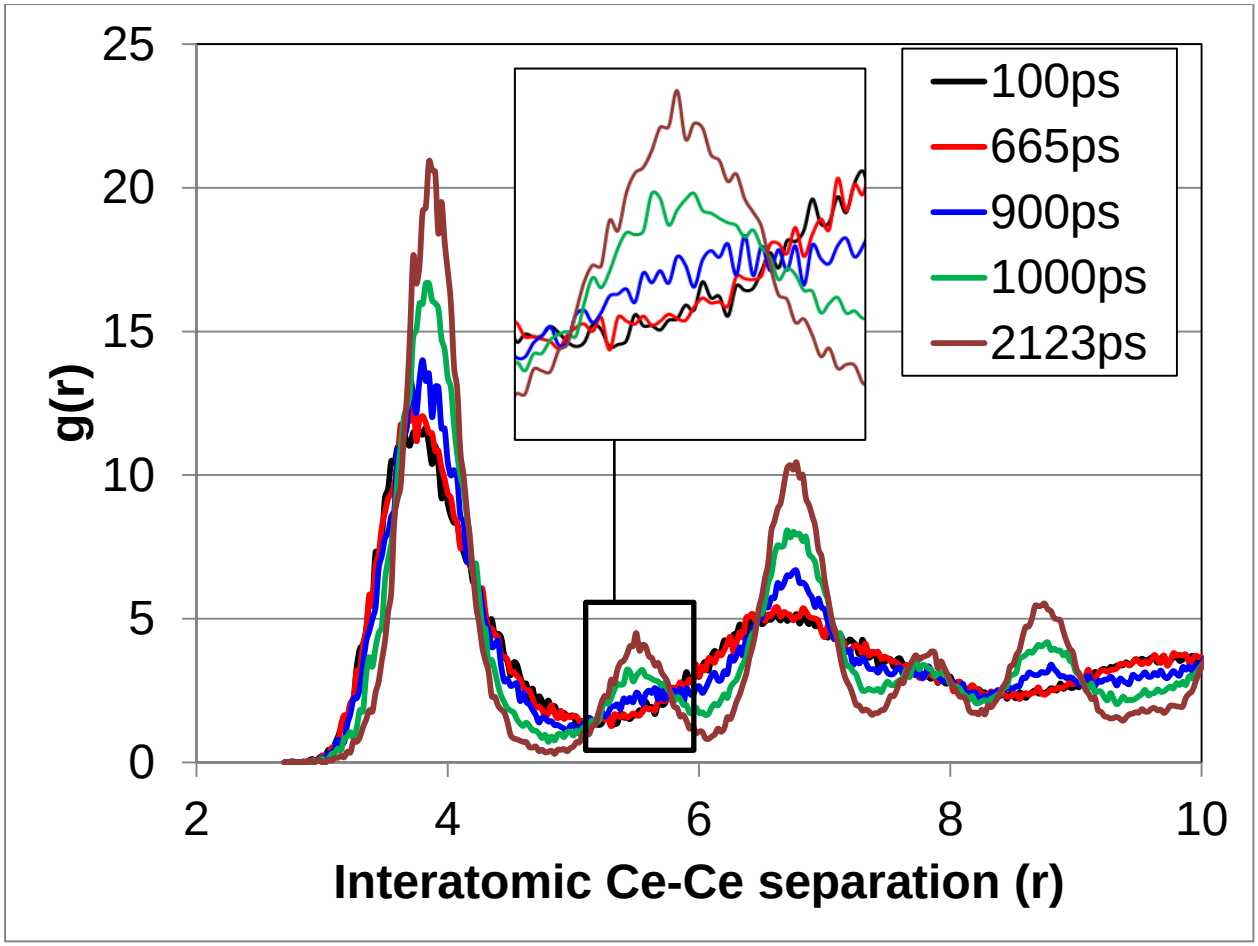

Figure 4 Ce-Ce Radial Distribution Functions, calculated as a function of time during the crystallisation and solidification of the ceria nanoparticle. Interatomic separations are shown in Å.

Propagation of Crystallisation The structure of the nanoparticle at 975ps, fig. 5(a), shows that almost all the cerium ions are ordered and located on (near) crystallographic lattice sites. However, in a shell comprising the nanoparticle, the oxygen ions are disordered (liquid-like), fig 5(b). The simulations reveal that crystallisation proceeds with the cations locating first to lattice sites and then the anions move to their respective lattice sites. Such crystallisation mechanisms are the same for all time periods in that as the crystallisation front emanates radially from the seed, the cerium sublattice crystallises first, followed by the oxygen ions. In particular, the ions 'pre-order' in the liquid phase and then solidify in this ordered state.

Physical Chemistry Chemical Physics Accepted Manuscript

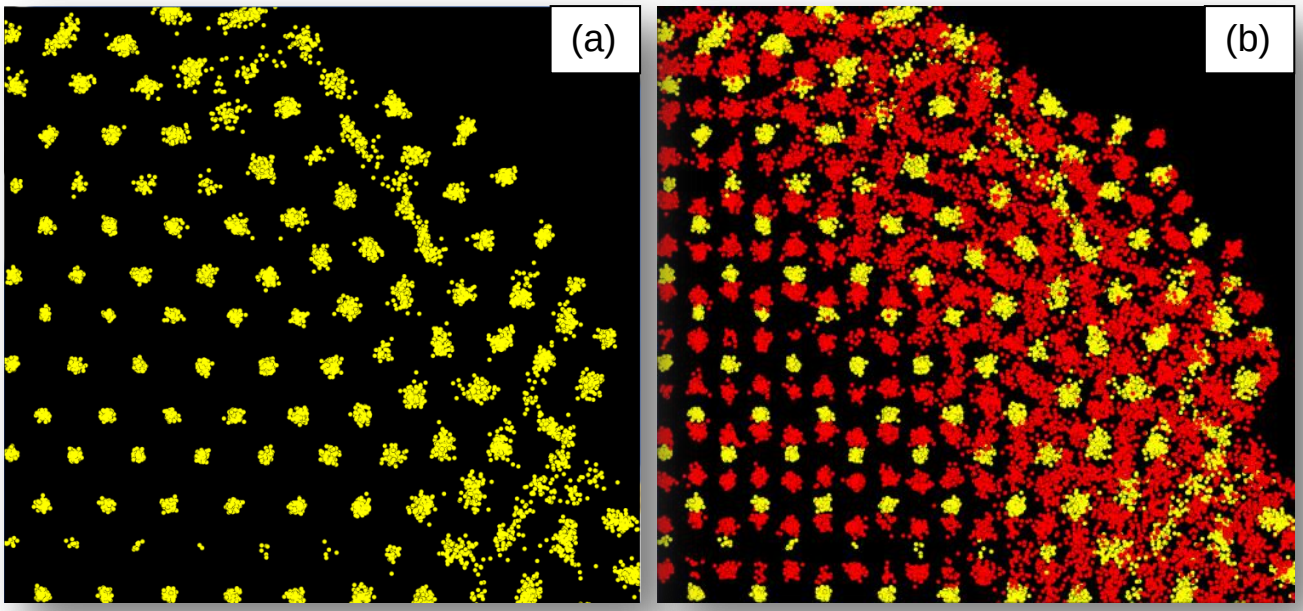

Figure 5 Atom positions comprising the ceria nanoparticle at 975ps. (a) Only cerium sublattice positions shown, (b) cerium and oxygen positions shown. Ce ions are coloured yellow and oxygen is red.

During crystallisation, point defects – including oxygen and cerium vacancies - evolve as a consequence of ions failing to occupy all available lattice sites. During the simulation, the oxygen vacancies are subsequently annealed out of the structure. In particular, the oxygen ions move, via a vacancy mechanism, to fill vacant positions. The mobility is concerted, with many oxygen ions moving at the same time. The pathways for the moving oxygen ions, together with the concerted movement can be seen in fig. 6. Most diffusion pathways are along <100>. However, there are a few jumps that occur along <110>; the latter is highlighted in the circle in fig 6(b). Conversely, once solid, the cerium ions are unable to move under MD simulation and the cerium vacancies become trapped within the (model) structure.

Physical Chemistry Chemical Physics Accepted Manuscript

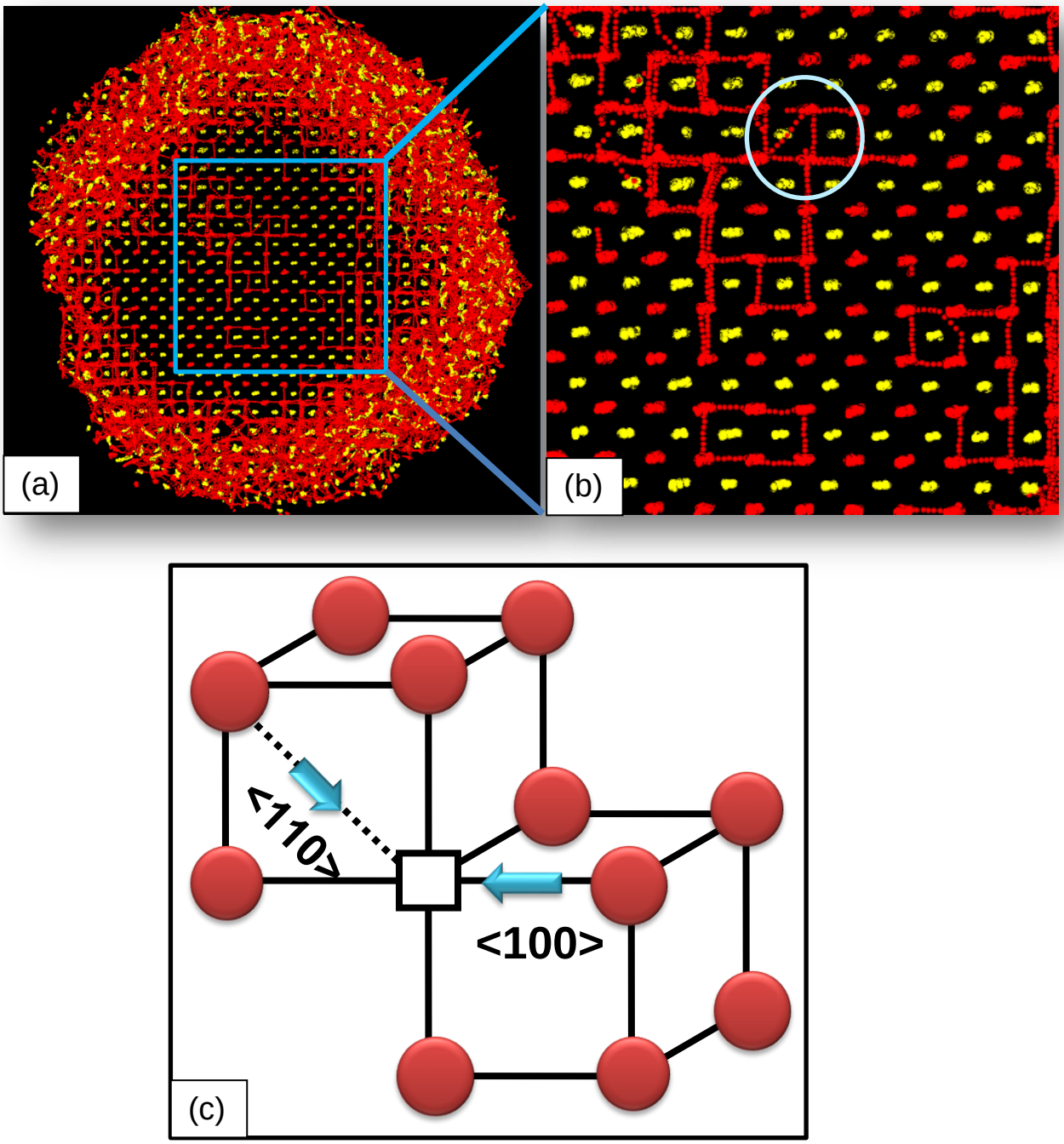

Figure 6 *Structure of the CeO_2 nanoparticle at 975ps showing the oxygen diffusion mechanism. (a) Slice cut through the whole ceria nanoparticle. (b) Enlarged segment of (a) showing more clearly the diffusion pathways. (c) Schematic showing the diffusion pathways along <100> and <110> in the idealised fluorite structure. Cerium ion positions are coloured yellow and oxygen is red.*

Physical Chemistry Chemical Physics Accepted Manuscript

The final, low temperature, structure of the CeO_2 nanoparticle (inset fig. 1(a)) conforms to the fluorite crystal structure and comprises a polyhedral morphology with {111} surfaces truncated by {100} in accord with experiment.[13]

DISCUSSION

The evidence that supports the concept that the crystalline seed, which nucleates the liquid-solid phase change, evolves as a liquid (crystal) rather than a solid (crystal) includes:

● (Only) 3% of the total calculated latent heat of solidification is liberated after 25% of the nanoparticle has crystallised, fig 1.

● Cerium ions, comprising the (liquid) crystal seed, have the same mobility as cerium ions comprising the amorphous regions, fig 3.

● Cation mobility starts to reduce after 25% of the nanoparticle is crystalline, fig 3.

● Calculated RDF's reveal no long-range structure within the nanoparticle when 25% of the nanoparticle is (visibly) crystalline, fig 4.

● Long-range structure starts to emanate (within the RDF) after more than 25% of the nanoparticle is crystalline, fig 2 and fig 4.

The spontaneous evolution of a crystalline seed, which nucleates a phase change from liquid to crystalline solid is a rare event because the energy barriers associated with ions rearranging from an amorphous to a crystalline solid are high. Accordingly, the structural hypersurface cannot be explored, within the timescales typically accessible to MD simulation, to facilitate spontaneous evolution of a crystalline seed. It is therefore surprising that such events have been documented in the open literature.[19] This can be explained if the crystalline seed spontaneously evolves as a *liquid* enabling MD simulation to adequately explore the potential hypersurface and spontaneously evolve a crystalline seed because the energy barriers for ion mobility in a liquid are normally much lower than for a solid. In particular, simulated crystallisation, using MD, has been used to 'observe' the crystallisation of water,[11] Li_2O (inverse fluorite)[20], TiO_2 (rutile)[21], ZnS (wurtzite) [19], MgO (rocksalt) [19] and MnO_2 (pyrolucite)[22] via the spontaneous evolution of a crystalline seed. Accordingly, we propose that nucleation of the liquid-solid phase change, via 'liquid' crystal seeds, is a more general phenomenon, applicable to other materials spanning several structural classes.

Physical Chemistry Chemical Physics Accepted Manuscript

CONCLUSION

Molecular dynamics, which was used to simulate directly the crystallisation of a ceria nanoparticle, reveals that the mechanism associated with the liquid to solid (crystal) phase change is a two-step process. First, the amorphous liquid spontaneously evolves into a crystalline liquid, and then the crystalline solid emanates from within the liquid (crystal) phase. Propagation of crystallisation proceeds via the cations locating first to lattice sites surrounded by a sea of liquid oxygen ions; the oxygen anions then locate to their respective lattice sites.

ACKNOWLEDGEMENTS

EPSRC: EP/H001220/1

REFERENCES

[1] Gebauer,D.; Kellermeier, M.; Gale, J. D.; b Lennart Bergstrom, L., and Colfen, H.
Pre-nucleation clusters as solute precursors in crystallisation
Chem. Soc. Rev., 2014, 43, 2348—2371

[2] Li, Y., and Shen, W.
Morphology-dependent nanocatalysts: Rod-shaped oxides
Chem. Soc. Rev., 2014, 43, 1543—1574

[3] Zhu. T., and Li, J.
Ultra-strength materials
Progress in Materials Science, 2010, 55, 710–757

[4] Malavasi, L.; Fisher, C. A. J., and Islam, M. S.
Oxide-ion and proton conducting electrolyte materials for clean energy applications: structural and mechanistic features
Chem. Soc. Rev., 2010, 39, 4370–4387

[5] McFarland, E. W., and Metiu, H.
Catalysis by Doped Oxides
Chem. Rev. 2013, 113, 4391−4427

[6] Piana, S.; Reyhani, M., and Gale, J. D.
Simulating micrometre-scale crystal growth from solution
Nature, 2005, 438, 70-73.

[7] On Structure and Properties of Amorphous Materials
Stachurski, Z. H.
Materials, 2011, 4, 1564-1598

[8] Song, R.-Q.; Colfen, H.; Xu, A.-W.; Hartmann, J., and Antonietti, M.
Polyelectrolyte-Directed Nanoparticle Aggregation: Systematic Morphogenesis of Calcium Carbonate by Nonclassical Crystallization
ACS Nano, 2009, 3, 1966–1978

[9] Xiang, B., Hwang, D. J., In, J. B., Ryu, S. G., Yoo, J. H., Dubon, O., Minor, A. M., and Grigoropoulos, C. P.
In Situ TEM Near-Field Optical Probing of Nanoscale Silicon Crystallization

Physical Chemistry Chemical Physics Accepted Manuscript

Nano Lett., 2012, *12*, 2524–2529

[10] Anwar, J. and Zahn, D.,
Uncovering Molecular Processes in Crystal Nucleation and Growth by Using Molecular Simulation
Angew. Chem. Int. Ed. 2011, 50, 2–20

[11] Molecular dynamics simulation of the ice nucleation and growth process leading to water freezing
Matsumoto, M.; Saito, S., and Ohmine, I.
NATURE , 2002, 416, 409-413

[12] Streitz, F. H.; Glosli, J. N.; Patel, M. V.; Chan, B.; Yates, R. K.; Supinski, B. R.; Sexton, J., and Gunnels, J. A.
Simulating Solidification in Metals at High Pressure: The Drive to Petascale Computing
Journal of Physics: Conference Series, 2006, 46, 254–267

[13] Feng, X. D.; Sayle, D. C.; Wang, Z. L.; Paras, M. S.; Santora, B.; Sutorik, A. C.; Sayle, T. X. T.; Yang, Y.; Ding, Y.; Wang, X. D., and Her, Y. S.
Converting ceria polyhedral nanoparticles into single-crystal nanospheres
Science, 2006, 312, 1504-1508

[14]Freeman, C. L.; Harding, J. H.; Quigley, D., and Rodger, P. M.
Structural Control of Crystal Nuclei by an Eggshell Protein
Angew. Chem. Int. Ed. 2010, 49, 5135 –5137

[15] Reed, K., Cormack, A., Kulkarni, A., Mayton, Sayle, D. C., Klaessig, F., and Stadler, B.,
Exploring the Properties and Applications of Nanoceria: Is There Still Plenty of Room at the Bottom?
Environ. Sci.: Nano, 2014, DOI: 10.1039/C4EN00079J

[16] Kumar, A., Das, S., Munusamy, P., Self, W. T., Baer, D. R., Sayle, D. C. and Seal, S.
Behavior of nanoceria in biologically-relevant environments
Environ. Sci.: Nano, 2014, DOI:10.1039/C4EN00052H.

[17] Sayle, T. X. T., Cantoni, M., Bhatta, U. M., Parker, S. C., Hall, S. R., Moebus, G., Molinari, M., Reid, D., Seal S., and Sayle, D. C.
Strain and Architecture-Tuned Reactivity in Ceria Nanostructures; Enhanced Catalytic Oxidation of CO to CO_2
Chem. Mater., 2012, 24, 1811−1821

[18] Smith, W., and Todorov, I. T.
A short description of DL_POLY
Mol. Simul., 2006 32, 935-943

[19] Sayle, D.C., Seal, S., Wang, Z. W., Mangili, B. C., Price, D. W., Karakoti, A. S., Kuchibhatla, S. V. T. N., Hao, Q., Möbus, G., Xu, X., and Sayle, T. X. T.
Mapping Nanostructure: A Systematic Enumeration of Nanomaterials by Assembling Nanobuilding Blocks at Crystallographic Positions
ACS Nano, 2008, 2, 1237–1251

[20] Sayle, T. X. T., Ngoepe, P. E., and Sayle, D. C.,
J. Mater. Chem., 2010, 20**,** 10452-10458

[21] Sayle, D. C., and Sayle, T. X. T.
High-Pressure Crystallisation of TiO_2 Nanocrystals
J. Comput. Theor. Nanos.,2007, 4, 299-308

[22] Sayle, T. X. T., Catlow, C. R. A., Maphanga, R. R., Ngoepe, P. E., and Sayle, D. C.
Modelling MnO_2 Nanoparticles using Simulated Amorphisation and Recrystallisation
J. Am. Chem. Soc., 2005; *127*, 12828 - 12837

Physical Chemistry Chemical Physics Accepted Manuscript